



Studies on initial permeability and loss factor in Ni–Zn ferrites synthesized by oxalate precursors

N.D. Chaudhari^a, R.C. Kambale^c, J.Y. Patil^b, S.R. Sawant^a, S.S. Suryavanshi^{b,*}

^a Department of Electronics, Shivaji University, Kolhapur 416004, MS, India

^b Department of Physics, Solapur University, Solapur 413255, MS, India

^c Department of Physics, Shivaji University, Kolhapur 416004, MS, India

ARTICLE INFO

Article history:

Received 22 December 2009

Received in revised form 2 June 2010

Accepted 23 June 2010

Available online 1 July 2010

Keywords:

A. Magnetic materials

B. Chemical synthesis

D. Magnetic properties

D. Microstructure

ABSTRACT

$\text{Ni}_x\text{Zn}_{1-x}\text{Fe}_2\text{O}_4$ ferrites with ($X = 0.28$ – 0.40 in step of 0.2) have been synthesized by oxalate precursor method and investigated for their, initial permeability and loss factor measurements. Initial permeability has been observed to increase with the increase in Ni^{2+} up to $X = 0.32$, beyond which it decreases. The variation of initial permeability has been explained by considering the factors such as grain size, saturation magnetization and anisotropy constant. Thermal variation of initial permeability reveals a peak height in μ_r - T curves which tends to increase with increase in Ni^{2+} content. μ_r - T curves also exhibit thermal hysteresis, which reveals the inverse relationship between the difference in heating and cooling curves at which hysteresis falls between Hopkinson peak and T_c with value of initial permeability. Loss factor values are small which is attributed to high density of the samples and processing techniques.

© 2010 Elsevier Ltd. All rights reserved.

1. Introduction

Ni–Zn ferrite is extensively studied due to its remarkable magnetic properties and low production cost. Ni–Zn ferrite has been widely used in inductors and electromagnetic wave absorber that require high value of initial permeability [1]. Microstructure and magnetic properties of Ni–Zn ferrites are highly sensitive to the method of preparation, sintering conditions and amount of constituent's metal oxides, impurities or doping level [2]. Improvement of initial permeability is important for ferrites, which makes them technologically important materials. The method of preparation and conditions of sintering profoundly influence the magnitude of initial permeability [3].

Ni–Zn ferrites are commonly synthesized using conventional ceramic method which involves direct mixing of constituent's oxides. Prolonged heating at high temperature is partly disadvantageous as it leads to volatilization of some constituents such as Zn and Li giving rise to non-stoichiometric product [4,5]. In contrast, soft chemical route yields metastable product, with better control over stoichiometry, structure, particle size and phase purity [6]. Many workers have studied the magnetic properties of Ni–Zn ferrites with various substitution synthesized by ceramic method

[2,4,7–15] as well as soft chemical route [16–25] such as combustion, hydrothermal, citrate and sol–gel methods.

Improvement of initial permeability is possible by densification and improvement in grain size with the control of the microstructure. However, using chemical route, large grain size cannot be achieved as a result, the courses left for improvement of initial permeability is improvement of bulk density and reduction of crystal anisotropy. We, therefore, decided to synthesize the Ni–Zn ferrites by chemical route with an intention to improve initial permeability by achieving high-density material through small grain size.

2. Experimental details

The oxalates were synthesized by a method suggested by Wickham [26] and subsequently modified by Bremer et al. [27] for synthesis of Mn–Zn ferrites. The oxalate precursor for synthesis of ferrite has been widely employed and found convenient, since it yields a homogeneous product in short time [28]. Oxalates are generally preferred because of their low solubility; low decomposition temperature and fine particle yield [29]. Their prime advantage is in achieving intimate mixing on an atomic scale resulting in the formation of true solid solution [5]. This uniformity in starting materials favors the diffusion dependent formation of homogeneous spinel at low temperature. For each composition iron acetate was prepared by adding AR grade glacial acetic acid to

* Corresponding author. Tel.: +91 217 2744771; fax: +91 217 2744770.
E-mail address: ssuryavanshi@rediffmail.com (S.S. Suryavanshi).

the required quantity of iron metal powder and distilled water to make a solution. To avoid the oxidation of Fe II to Fe III, the entire reaction was carried out in CO₂ atmosphere instead in N₂ atmosphere [27].

Required quantity of nickel acetate, zinc acetate and iron acetate as synthesized above (total metal ion concentration = 0.45 M) were slowly added to ammonium oxalate solution (0.60 M) to precipitate the required oxalate in order to maintain the desired stoichiometry. Metal acetates are the best starting materials since they yield acetic acid as a by-product [30]. The above-synthesized acetates were slowly added to hot ammonium oxalate solution to precipitate the required oxalate complex which is then filtered and dried. In this manner, various oxalate complexes having the chemical formula Ni_xZn_{1-x}Fe₂(C₂O₄)₃·nH₂O where X = 0.28, 0.30, 0.32, 0.34, 0.36, 0.38, 0.40 were synthesized and decomposed at 623 K for 3 h. The decomposed powder obtained was used to prepare a toroid of OD = 2.5 cm and ID = 1 cm, by applying a pressure (1.07 × 10⁹ dyne/cm²). Final sintering was carried out in air atmosphere at 1323 K for 10 h followed by slow cooling.

The initial permeability measurements of toroid samples were taken using HP-4284 A LCR precision meter from room temperature to the Curie temperature at 1 kHz from low field inductance measurements of coils with toroidal cores using the relation:

$$\mu_i = \left[\frac{L}{0.0046N^2h \log d_2/d_1} \right]$$

where L is the inductance in μH ; N is the number of turns; d_2 is the outer diameter; d_1 is the inner diameter; h is the height of core in cm; μ_i is the initial permeability. The microstructural aspects were studied with a scanning electron microscope (SEM: model JEOL-JSM 6360). From SEM micrographs the grain size (D) was calculated by using the line intercept method.

3. Results and discussion

3.1. Compositional variation of μ_i

From Table 1 it is clear that the initial permeability increases with increase in Ni²⁺ content up to $X = 0.32$, thereafter it decreases with further addition of Ni²⁺. The values of corrected initial permeability (μ_{ic}), wall permeability (μ_w), rotational permeability (μ_{rk}), anisotropy constant (K_1), saturation magnetization (M_s), % density of sample (ρ_a) and grain size (D) are given in Table 1. The corrected initial permeability has been calculated using the relation given by Globus et al. [31]:

$$(\mu_i - 1)_c = (\mu_i - 1) \frac{dx}{da}$$

where $(\mu_i - 1)_c$ = corrected initial permeability, $(\mu_i - 1)$ = observed initial permeability, dx = X-ray density, and da = observed density of sample (xylene method).

The initial permeability is dependent on the intrinsic parameters mainly the saturation magnetization M_s and anisotropy

constant K_1 —which depends on the temperature and are specific to a given composition. The parameters of technological importance that govern μ_i are microstructure, grain size, stoichiometry, internal stress and crystalline defects.

In the present case, the variation of initial permeability (μ_i) with Ni²⁺ content can be explained by considering the variation of M_s , D and K_1 . From Table 1 it is clearly seen that the magnitude of wall permeability μ_w is large in comparison with the rotational permeability μ_{rk} , in all compositions. Thus it is concluded that the main contribution to the initial permeability is due to wall motion. Hence Globus model is applicable [31] for the present studies:

$$\mu_i = \frac{M_s^2 D_m}{K_1}$$

where D_m = average grain size, K_1 = anisotropy constant, and M_s = saturation magnetization.

The values of M_s are obtained from vibrating sample magnetometer (VSM) measurement and the values of (K_1) are calculated by taking the end values of the corresponding ferrites and taking into consideration the stoichiometry of the composition.

From Table 1, it is seen that with increasing Ni²⁺ content, M_s and K_1 both increase in magnitude, whereas the grain size does not exhibit a systematic trend. It is well known that the initial permeability increases linearly with increase in grain size. The linear relationship between μ_i and D is reported to be due to an increased bulging volume of domain wall and decreasing domain wall pinning by the grain boundaries with increasing grain size and thus diminished demagnetizing effects [31]. In present study, the initial permeability seems to be independent of grain size and hence the effect of grain size has not been considered. As such M_s and K_1 have been considered to be responsible for the observed variation of μ_i . From the Globus relation, it is understood that initial permeability varies as the square of saturation magnetization. From Table 1 it is seen that M_s increases as the content of Ni²⁺ increases. Ni–Zn system exhibits the Y–K type spin arrangement in which the Y–K angles goes on decreasing with addition of Ni²⁺, leading to increase in A–B interaction. Thus the change in magnetization occurs due to the presence of Y–K angles in the spin system on B site. Hence an increase in initial permeability initially up to $X = 0.32$ can be attributed to increase in M_s . K_1 also increases with the addition of Ni²⁺ which should tend to decrease μ_i . It however appears that effect of M_s on μ_i overtakes the effect of μ_i on K_1 and the overall effect is the increase of μ_i .

It is well known that the anisotropy makes definite contributions to the quantity like magnetic susceptibility, frequency of ferromagnetic resonance, permeability and hysteresis [32]. This is due to, the interaction between two magnetic dipoles and is dependent on the arrangement of the magnetic spins in the lattice and the nature of the magnetic ions. The spin orbit interaction of magnetic ions involved makes a definite contribution to the anisotropy. As a result of this interaction, the spin aligns themselves in a direction perpendicular to the plane of the orbits, which is fixed with respect to the crystal axis. Hence the

Table 1
Data on initial permeability (μ_i), wall permeability (μ_w), rotational permeability (μ_{rk}), grain size (D), % observed density (% ρ_a), anisotropy constant (K_1), saturation magnetization (M_s), loss factor (LF) and indication of thermal hysteresis (ΔT) for Ni_xZn_{1-x}Fe₂O₄ ferrite system.

X	μ_i	μ_w	μ_{rk}	D (μm)	% ρ_a	$-K_1 \times 10^3$ erg/cm ³	M_s (emu/gm)	LF $\times 10^{-5}$
0.28	1384	1220	164	–	99	1.3	36	0.99
0.30	1546	1363	183	0.84	96	1.6	42	0.85
0.32	1601	1412	189	0.73	97	1.9	47	0.78
0.34	1345	1186	159	0.91	96	2.6	49	1.1
0.36	1080	952	128	0.88	97	3.8	53	1.6
0.38	950	838	112	–	96	5.0	58	2.2
0.40	1030	902	128	–	95	5.8	61	1.96

magnetization along one of the crystal axis is preferred. These results in the increase of anisotropy energy, thus K_1 increases as nickel ferrite has the value of K_1 about $-6.3 \times 10^3 \text{ erg/cm}^3$. Thus the decrease of initial permeability can be attributed to the increase of anisotropy constant K_1 . At higher concentration of Ni^{2+} , μ_i decrease; this is so because K_1 changes by a large magnitude than M_s . Thus K_1 plays a predominant role in decreasing μ_i at higher concentration of Ni^{2+} .

It is known that the thickness and chemical composition of grain boundary are two critical factors in determining the magnetic properties of ferrites. The thickness of grain boundary affects the value of μ_i [33]. Samples of the same compositions with nearly same grain size are found to possess different values of μ_i because of the difference in non-magnetic grain boundary thickness. The thickness of grain boundary depends on the misfit which involves adjacent grains growing along different crystallite lattice orientations, thus generating large plastic strains at the grain boundaries disrupting the magnetic ordering and creating non-magnetic regions. For Li–Cd ferrites, Bellad et al. [34] have concluded that the increase in μ_i (when both M_s and D decreases) can be attributed to the decrease in thickness of non-magnetic grain boundary, which in turn decreases the domain wall energy and allows the easy movement of domain walls. The higher the grain boundary, higher will be the domain wall energy which in turn leads to higher values of anisotropy constant. In present case, the anisotropy constant K_1 goes on increasing with addition of Ni^{2+} indicating that the domain wall energy increases, hence it constrains free and easy domain wall motion. This reduces the magnitude of initial permeability at higher concentration of Ni^{2+} .

It is well known that the permeability of polycrystalline ferrites can be described as the superpositions of two mechanisms, i.e. spin rotation and domain wall motion [35]. The values of rotational permeability and wall permeability have been calculated using the formulae [36]:

$$\mu_{rk} = 1 + \frac{2\pi M_s^2}{K_1}$$

$$\mu_w = \mu_i - (\mu_{rk} - 1)$$

where M_s = saturation magnetization, K_1 = anisotropy constant; μ_{rk} = rotational permeability, and μ_w = wall permeability.

From Table 1, it is seen that the magnitude of wall permeability is very large in comparison with the rotational permeability in all the compositions. Globus et al. [31,37] proposed a model, which could account for observed linear dependence of initial permeability and grain size. In this model, permeability due to wall motion was linearly dependent on grain size while permeability contribution due to spin rotation was independent of grain size. In present data, there is no systematic variation in grain size and initial permeability with increase in Ni^{2+} content. But from the values of wall and rotational permeability, the contribution to initial permeability is seen to be due to domain wall motion.

3.2. Microstructure

The SEM photograph of selected composition, which exhibits high value of initial permeability in the system $\text{Ni}_x\text{Zn}_{1-x}\text{Fe}_2\text{O}_4$ is shown in Fig. 1. The following observations have been made:

- (1) The grains are not separated by a large margin suggesting that the intergranular porosity is minimum which is clear from the high-density values of these compositions.
- (2) The permeability does not exhibit one to one correspondences with the grain size; further the grain size does not show any particular trend with increasing Ni^{2+} content.
- (3) The grain size is very small, i.e. $<1 \mu\text{m}$.
- (4) There is a clear distribution in grain size.

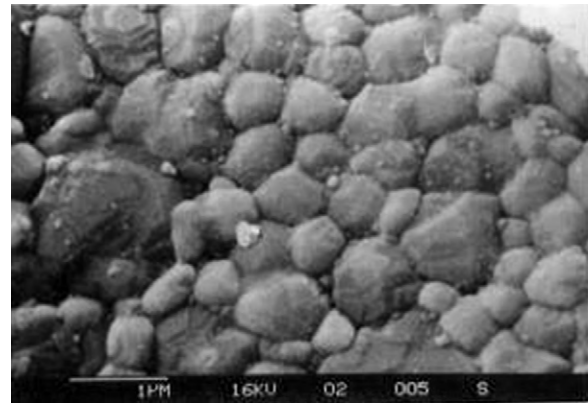


Fig. 1. SEM photograph for Ni–Zn ferrites $X = 0.32$.

In the present compositions, the low values of porosity (3–4%) or full densification appears to be due to the fine particle nature exhibited by ferrite composition under consideration. In order to obtain a low porosity, it is useful to promote sintering rate by using powders with large surface area and such a sintered reactive powders are obtained from wet chemical preparation method such as co precipitation technique. They have low porosity, high densification and small grain size which are attributable to the processing technique.

The ferrite composition with $X = 0.32$ which exhibit high value of initial permeability and high density. However, the grain size for this sample is low. The density values of the present samples are of the order 96–97%, whereas their grain size ranges from 0.73 to 0.91 μm . There is no definite trend for variation of grain size and density with increasing Ni^{2+} content. Also the permeability does not exhibit the linear dependence of grain size. But the values of initial permeability are above 1000 for all the compositions. Li [38] examined the samples of Ni–Zn ferrites from two commercial sources and found the scatter in grain size dependency at small grain size and better linearity at larger grain size. The relationship between permeability and grain size will be generally linear only, if grain growth is normal that is if all the grains grow pretty much at the same time and same rate. This leads to a rather narrow range of final grain size.

3.3. Thermal variation of μ_i

Thermal and frequency variation of initial permeability (μ_i) furnish valuable information about domain nature [39], Curie temperature [40] and factors contributing to permeability [41]. Many workers [7,8,14,41a] have explored the behavior of μ_i as a function of temperature. The parameters such as M_s , D and K_1 are responsible for the diversity of the thermal spectra of μ_i of the ferrite sample. In present study, the variation of μ_i as a function of temperature in the range from room temperature to the Curie temperature have been shown in Fig. 2(a)–(g). The following observations have been made:

- (1) For the compositions with $X = 0.28, 0.30, 0.32, 0.34$:
 - (a) There is no peaking behavior in μ_i – T variation.
 - (b) The permeability does not change with temperature up to the certain temperature.
 - (c) Initial permeability drops with temperature near T_c and becomes zero at T_c .
 - (d) All the compositions are single phase as double T_c or gradual variation of μ_i with T has not been observed.

For these above compositions, the initial permeability does not change with temperature up to certain temperature. This

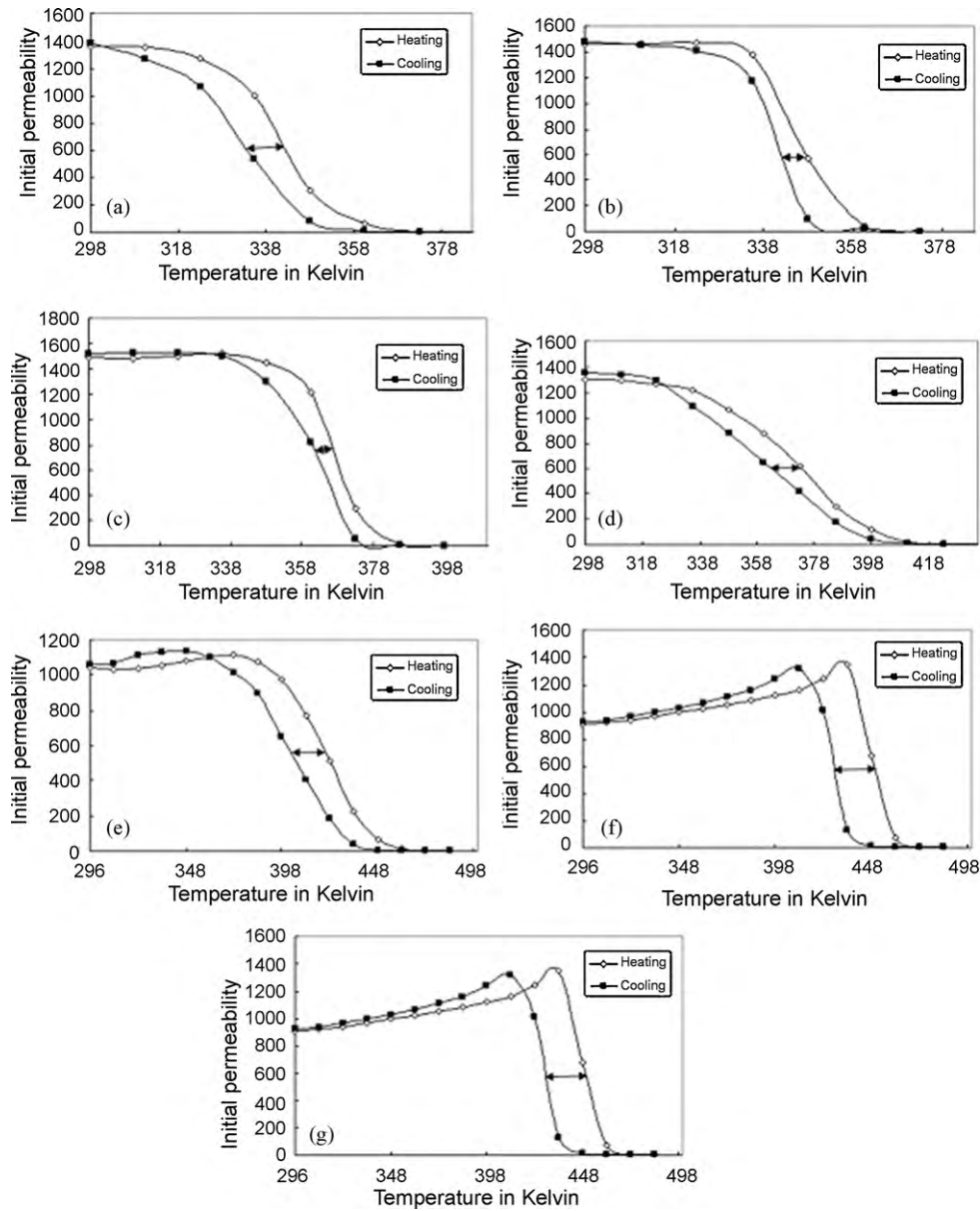


Fig. 2. (a–g) Thermal variation and thermal hysteresis of initial permeability for Ni–Zn ferrite system.

behavior is explained by considering the compensating effects in M_s and K_1 with temperature. Kakatkar et al. [3] have reported μ_i - T curves for Ni–Zn ferrites and observed a very small decrease in μ_i over the temperature range of their experiment. They have attributed this behavior to the compensating effects in M_s and K_1 with temperature, however the shape of the curves was not affected by the addition of Zn^{2+} (except the magnitude of μ_i). Similar behavior of μ_i - T curves have been reported by Sankpal et al. [42], they have not noticed any profound peaking behavior in μ_i - T variation. They have attributed this behavior to the rate of change of M_s and that of anisotropy field with temperature is the same. This type of peak may be below the room temperature region and some workers [24,25] have observed such a peak. Thus for these composition, it can be concluded that the peaking behavior is absent due to the anisotropy constant K_1 which does not change its sign within the temperature range of the experiments.

(2) For the compositions with $X = 0.36, 0.38, 0.40$:

(a) The initial permeability increases slowly with temperature and exhibits a peak near the Curie temperature.

(b) The peak height increases with the increase of Ni^{2+} content.

(c) The peaking temperature increases on the addition of Ni^{2+} content.

(d) Near T_c , μ_i fall rapidly and become zero at Curie temperature. The sharp fall suggests the single-phase formation of ferrite material. Many workers [42,34] have reported similar observation and conclusions.

In the above compositions, increase of μ_i with temperature can be explained as follows.

The anisotropy constant and saturation magnetization usually decrease with the increase in temperature due to the thermal agitation, which disturbs the alignment of magnetic moments [43]. But the decrease of K_1 with temperature is much faster than M_s [44]. When K_1 goes through zero, μ_i attain its maximum value and then drop to zero above T_c .

The peak height increases with the increase of Ni^{2+} content which can be related to the rate of change of M_s and K_1 with temperature. The increase in Ni^{2+} content results in net increase in magnetic moment, which leads to increase in anisotropy constant.

Thus peak height increases with increase in Ni^{2+} content. Drofenik [45,46] has reported that the distant pores rather than the grain size account for the variation in permeability. Samples with giant grain and induced porosity owing to exaggerated grain growth still had higher permeability's than those with normally grown grains, provided the distance between pores were the same and concluded that the large grained samples were less sensitive to grain boundary effects and thus the μ versus T curve was more peaked. Thus for these compositions, it can be concluded that the peak in μ_i - T variation are due to change in sign of K_1 .

3.4. Thermal hysteresis in μ_i - T curves

Loeac [47] has classified thermal spectra of μ_i into two categories as follows: (1) Ferrites exhibiting one peak in μ_i called Hopkinson peak near T_c followed by steady decrease of μ_i with increasing temperature. (2) Ferrites exhibiting an additional peak at lower temperature.

Loeac classified two types of hysteresis on the basis of his observations are

- (1) Far below T_c , permeability obtained during heating is always lower than that of obtained during cooling.
- (2) Between the Hopkinson peak and T_c , the heating curve is beyond cooling one. He attributed this thermal hysteresis to domain wall topography.

From the thermal hysteresis curve of present ferrite system (Fig. 2), the following observations have been made:

- (1) Two types of hysteresis are observed—first is below T_c and second one is between Hopkinson peak and T_c .
- (2) Permeability obtained during heating is lower than that obtained during cooling, indicating that M_s and K_1 changes differently with respect to temperature during cooling and heating.
- (3) Peak in μ_i - T variations during heating cycle occurs at a higher temperature than that observed during cooling cycle, indicating that K_1 changes its sign at two different temperatures.
- (4) The μ_i - T variation also shows two slopes in the region where the heating begins. This may be due to different rates of change of M_s and K_1 with respect to temperature.
- (5) All μ_i - T curves clearly indicate the inverse relationship between the variation of difference in heating and cooling curves at which hysteresis falls between Hopkinson peak and T_c with the value of μ_i . It has been already concluded that the peak in μ_i - T variation is attributable to the sign of K_1 . Two different paths of μ_i , one during heating and other during cooling indicates that the values of K_1 and M_s during heating and during cooling are different ultimately leading to the hysteresis effect. The slopes of μ_i - T curves near T_c appear to be the same.
- (6) Permeability curves during heating cycle and that during cooling cycle meet each other at a point called the crossing point which tends to increase with increase of T_c and Ni^{2+} content. This point signifies the fact that the rates of variation of M_s and K_1 with respect to temperature are identical during heating and cooling cycles.

Globus and Duplex [48] explained hysteresis I as follows—when cooling from T_c , near the Hopkinson peak, K_1 is at first small and as M_s increases more rapidly, it is easy for the magnetization and the domain walls to align themselves along the director circles of torus. At lower temperatures, where K_1 is large and the easy directions in such a way that the alignment becomes worse

influence the topography of the domain walls. So the values of permeability is lower than that due to ideal toroidally symmetrically configuration. On heating the sample again from this low temperature, the pinning forces tend to maintain the domain walls in their previous positions. Therefore the alignment is not as good as that during the cooling run involving the hysteresis characterized by lower value of μ_i .

Loeac [49] has explained the hysteresis II as follows; the hysteresis appearing in the vicinity of T_c can also be explained by the effect of competition between M_s and K_1 on the alignment of the domain walls. For this he considered the decrease of temperature from above T_c . On crossing the transition point, the material is magnetized spontaneously and this is accompanied by the appearance of domain walls. At that temperature, both M_s and K_1 are small and there is no contribution favorable to the alignment of the domain walls and as each grains has three or four easy axes according to the sign of K_1 . The domain walls remain relatively disordered until the increasing M_s tend to align them. This also explains the Hopkinson peak, which could correspond to the best alignment before the increasing influence of K_1 .

Approaching T_c during the heating run, on the other hand, the material returns from the situation (Hopkinson peak) where both K_1 and M_s are decreasing but the domain walls have previously been aligned by high M_s . At a certain temperature between Hopkinson peak and T_c this situation is more favorable to a higher permeability, leading to hysteresis. The explanations put forward by these workers are applicable to our materials, since the observations are similar.

3.5. Frequency variation of μ_i

Variation of μ_i with frequency in the range 20 Hz to 1 MHz is shown in Fig. 3. It is seen that the initial permeability is almost constant and increases sharply at higher frequency except for the little variation at low frequency. The major contribution to μ_i is due to domain wall motion, which is manifested here by the low frequency dispersion effect observed. The occurrence of dispersion and absorption at frequencies in the region of 1 MHz was first established experimentally by Snoek, who attributed the phenomenon to the spin resonance in the internal anisotropy field. Rado and his co-workers believed that the absorption observed at higher frequency which is attributable to rotational resonance in the combined anisotropy-demagnetizing field. They attributed the lower frequency region to domain wall displacement, which they believed to make the major contribution to the initial permeability.

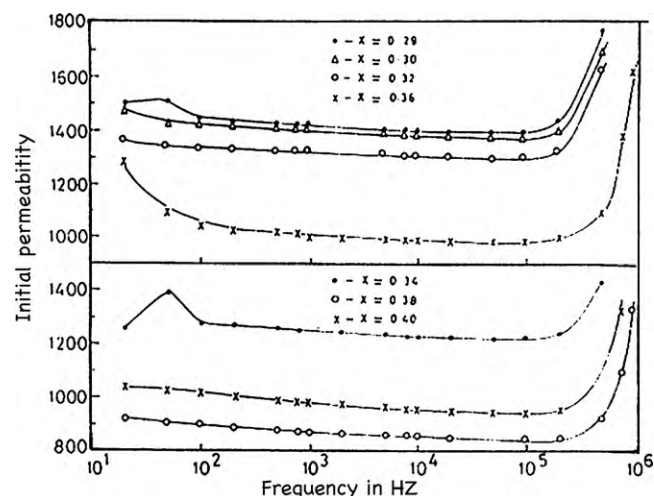


Fig. 3. Frequency variation of initial permeability.

In the present ferrite system, the dispersion at higher frequency is attributable to spin resonance in the internal anisotropy field and that at lower frequency to the major contribution of domain wall motion to the initial permeability. Similar results were concluded by Sankpal et al. [42].

3.6. Loss factor

Loss factor is defined as $LF = \tan \delta/\mu_i$. This parameter should be as low as possible, because the ferrites were almost exclusively used as a core material for coil carrying low level power and having as their main characteristics, a low loss factor [49].

Some workers [42,18] have reported work on loss factor. Recently Anilkumar et al. [18] have shown that the frequency, at which the loss factor gives a minimum, strongly depends on the microstructural features of Ni–Zn ferrites.

From Table 1, It is seen that the loss factor first decreases with the addition of Ni^{2+} up to $X=0.32$ and thereafter it increases. As Ni^{2+} content is increased, the net magnetic moment of resulting system increases. The magnetic energy applied to the substance will orient the magnetic moment vector towards the preferred easy direction. As a result, the some of magnetic energy is lost or not utilized in orienting the magnetic moment vectors, hence the loss factor arise. With increasing Ni^{2+} content, the net magnetic moment increases, majority of magnetic energy is utilized in orienting the magnetic moment towards easy direction, hence the loss factor shows decreasing trend initially. For $X=0.32$, loss factor is least whereas initial permeability is highest. For this composition, the net magnetic moment is maximum hence out of total magnetic energy, small amount of energy is lost, and hence the loss factor has least value. Beyond $X=0.32$, loss factor increases, whereas initial permeability value shows decreasing trend, in this region the rate of increase of K_1 is faster than that of M_s , hence out of the applied magnetic energy, less energy is utilized in orienting magnetic moments towards easy direction, thus there is more loss of magnetic energy. In other words, the loss factors values increases, with increase in Ni^{2+} content. The loss factor has very small values, which may be due to very small grain size and high density of the samples. Low value of loss factor is exhibited by the ferrite compositions $X=0.32$, this composition also exhibit high value of initial permeability and very small grain size, indicating that the loss factor depends on the grain size of the sample.

The variation of loss factor with temperature for the present ferrite system is shown in Fig. 4. It is seen that, the loss factor tends to increase slowly with the increase of temperature at lower content of Ni^{2+} and in lower temperature. At higher content of Ni^{2+} ,

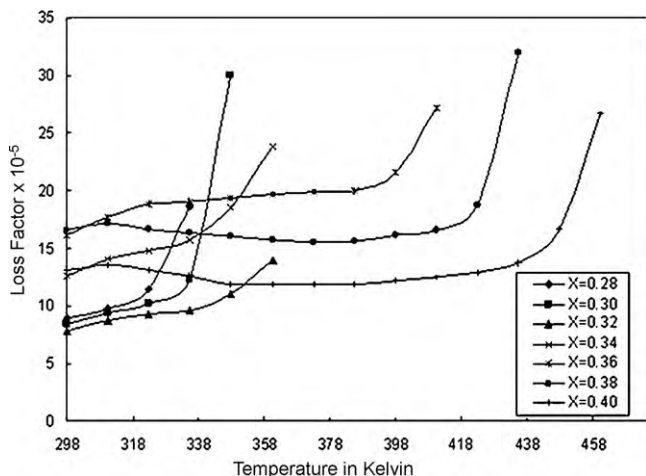


Fig. 4. Variation of loss factor with temperature for Ni–Zn ferrite system.

loss factor is invariant with increasing temperature. At higher temperature, loss factor shows increasing trend. This increase in loss factor is due to thermal randomization of domains. The increase in temperature weakens the exchange forces between the domains, due to this domain orient in random manner; this ultimately results in phase transition from ferrimagnetic to paramagnetic at Curie point. As temperature is increased, the exchange forces get weakened due to which domain starts orienting in random direction hence the loss factor increases initially and when all the domains are oriented in random direction the phase transition occurs. Almost all domains are randomly oriented.

In Fig. 5, the variation of loss factors with frequency in the range 20 Hz to 1 MHz shown. It is seen that the loss factor decreases with increase in frequency and attains a minimum value in the range of 50 to 100 kHz and at higher frequency the loss factor increases. Kramer and Panova [50] explained that the increase of loss factor at higher frequency is attributed to the phenomenon of domain wall relaxation which involves the hindrance to the domain wall motions of small grains by those of large grains where the later type of grains are small in numbers. The occurrence of high value of loss factor at lower frequency is due to the different types of wall relaxation processes [51]. It is assumed that the magnetic energy levels of a magnetic ion depend on the orientation of the magnetization for each orientation there exists equilibrium Boltzman distribution. In the moving wall the magnetization

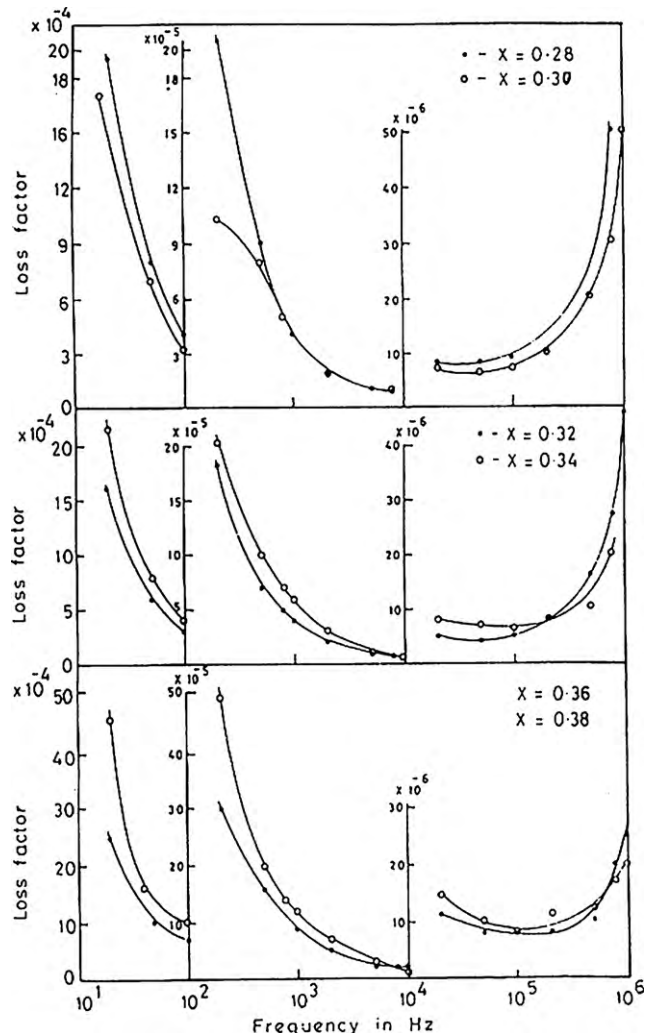


Fig. 5. Frequency variation of initial permeability for Ni–Zn ferrite system.

changes its directions and hence the energy levels, resulting in the change in redistribution that occurs in a finite relaxation time τ , causing the magnetization to lag behind the applied field. The maximum loss occurs at a frequency $\tau = 1/\omega$, which is proportional to the conductivity [52]. Our observed variation appears to follow the similar behavior.

4. Conclusion

$\text{Ni}_x\text{Zn}_{1-x}\text{Fe}_2\text{O}_4$ ferrites with $X = 0.28, 0.30, 0.32, 0.34, 0.36, 0.38$ and 0.4 have been successfully synthesized by employing oxalate precursor method. Initial permeability measurements reveals that it increase with increase in Ni^{2+} up to $X = 0.32$, and thereafter decreases. Thermal variation of initial permeability indicates that peak height in μ_i-T curves increases with increase in Ni^{2+} content. μ_i-T curves exhibits a thermal hysteresis, which reveals the inverse relationship between the difference in heating and cooling curves at which hysteresis falls between Hopkinson peak and T_c with value of initial permeability. The studies on loss factor show decreasing trend with the addition of Ni^{2+} up to $X = 0.32$ and thereafter it increases.

Acknowledgement

One of the authors, Dr. N.D. Chaudhari gratefully acknowledges financial assistance under UGC (University Grant Commission) New Delhi, India. One of the authors, Mr. R.C. Kambale is grateful to the Council of Scientific and Industrial Research (CSIR) of Human Resource Development Group, New Delhi, Government of India, for providing the financial support to carry out this research work through Senior Research Fellowship.

References

- [1] T. Tsutaoka, J. Appl. Phys. 93 (2003) 2789.
- [2] O.F. Caltun, L. Spinu, IEEE Trans. Magn. 37 (2001) 2353.
- [3] S.V. Kakatkar, S.S. Kakatkar, R.S. Patil, A.M. Sankpal, N.D. Chaudhari, P.K. Maskar, S.S. Suryavanshi, S.R. Sawant, Mater. Chem. Phys. 46 (1996) 96.
- [4] R. Peelamedu, C. Grimes, D. Agrawal, R. Roy, P. Yodoji, J. Mater. Res. 18 (2003) 2292.
- [5] K.C. Patil, S. Sundermanmohan, D. Gajapathy, in: N.P. Cheremisinoff (Ed.), Handbook of Ceramics and Composites, vol. 1, Marcel Dekker, NY, 1990, p. 469.
- [6] C.N. Rao, Chemical Approaches to the Synthesis of Inorganic Materials, Wiley Estem./Age Inter., New Delhi, 1993.
- [7] E. Rezlescu, N. Rezlescu, C. Posnicu, M.L. Crauss, Ceram. Int. 19 (1993) 71.
- [8] N. Rezlescu, E. Rezlescu, Solid State Commun. 88 (1993) 139.
- [9] R.K. Puri, R. Mitra, R.G. Mendiratta, Cryst. Prop. Prep. 27 (1989) 353.
- [10] A.M. Abden, J. Magn. Magn. Mater. 185 (1998) 199.
- [11] S.V. Kakatkar, S.S. Kakatkar, R.S. Patil, A.M. Sankpal, S.S. Suryavanshi, D.N. Bhosale, S.R. Sawant, Phys. Status Solidi B 198 (1996) 853.
- [12] A.M. Sankpal, S.S. Suryavanshi, S.V. Kakatkar, G.G. Tenshe, R.S. Patil, N.D. Chaudhari, S.R. Sawant, J. Magn. Magn. Mater. 186 (1998) 349.
- [13] M.C. Sable, B.K. Labde, N.R. Shamkumar, Bull. Mater. Sci. 28 (2005) 35.
- [14] A.A. Sattar, H.M. El-Sayed, K.M. El-Shokrofy, M.M. El-Tabey, J. Appl. Sci. 5 (2005) 162.
- [15] H. Su, H. Zhang, X. Tang, X. Xiang, J. Magn. Magn. Mater. 2 (2004) 157.
- [16] T.T. Shrinivasan, R. Ravindranathan, L.E. Cross, R. Roy, R.E. Newhan, S.G. Sankar, K.C. Patil, J. Appl. Phys. 63 (1988) 3789.
- [17] P.S. Anilkumar, J.J. Shrotri, S.D. Kulkarni, C.E. Deshpande, S.K. Date, Mater. Lett. 27 (1996) 293.
- [18] P.S. Anilkumar, J.J. Shrotri, C.E. Deshpande, S.K. Date, J. Appl. Phys. 81 (1997) 4788.
- [19] P. Ravindranathan, K.C. Patil, Am. Ceram. Soc. Bull. 66 (1987) 668.
- [20] P.S. Anilkumar, J.J. Shrotri, S.D. Kulkarni, C.E. Deshpande, S.K. Date, Asian J. Phys. 6 (1997) 217.
- [21] A. Verma, T.G. Goel, R.G. Mendiratta, P. Kishan, J. Magn. Magn. Mater. 208 (2000) 13.
- [22] W.C. Kim, S.I. Park, S.J. Kim, S.W. Lee, C.S. Kim, J. Appl. Phys. 87 (2000) 6241.
- [23] A.K. Singh, T.G. Goel, R.G. Mendiratta, O.P. Thakur, C. Prakash, J. Appl. Phys. 92 (2002) 3872.
- [24] S.A. Morrison, C.L. Cahill, E.E. Carpenter, S. Calvin, R. Swaminathan, M.E. Mottentry, V.G. Haris, J. Appl. Phys. 95 (2004) 6392.
- [25] C. Caizer, M. Stefanescu, J. Phys. D: Appl. Phys. 35 (2002) 3035.
- [26] D.G. Wickham, Inorg. Synth. 9 (1967) 152.
- [27] M. Bremer, St. Fisher, H. Langbein, W. Topelmann, H. Scheler, Thermochim. Acta 209 (1992) 323.
- [28] D.N. Bhosale, N.D. Chaudhari, S.R. Sawant, P.P. Bakare, J. Magn. Magn. Mater. 173 (1997) 51.
- [29] M. Paulus, in: P. Hagnemular (Ed.), Preparative Methods in Solid State Chemistry, Academic Press, NY, 1972, p. 487.
- [30] F.K. Lotergering, Philos. Res. Rep. 11 (1956) 337.
- [31] A. Globus, P. Duplex, M. Guyot, IEEE Trans. Magn. 7 (1971) 617.
- [32] V.R.K. Murthy, B. Vishwanathan, Science and Technology, Narosa Publication House, Bombay, 1990.
- [33] E.G. Visser, M.T. Johnson, P.J. Vander Zaag, in: Proceedings of the 6th International Conference on Ferrites, Japan, (1992), p. 807.
- [34] S.S. Bellad, S.C. Watwe, B.K. Chaugule, J. Magn. Magn. Mater. 195 (1999) 57.
- [35] S. Chikazumi, Physics of Magnetism, Wiley, NY, 1966.
- [36] K.J. Standely, Oxide Magnetic Materials, Clarendon Press, NY, 1971.
- [37] A. Globus, M. Guyot, Phys. Status Solidi B 52 (1972) 427.
- [38] X.S. Li, IEEE Trans. Magn. MAG-22 (1986) 14.
- [39] C.R.K. Murthy, S.D. Likhite, E.J. Deutch, G.S. Murthy, Phys. Earth Planet Int. 30 (1982) 287.
- [40] S.R. Jadhav, S.R. Sawant, S.S. Suryavanshi, S.A. Patil, J. Less Commun. Met. 158 (1990) 199.
- [41] (a) S.A. Mazen, S.F. Mansour, H.M. Zaki, Cryst. Res. Technol. 38 (2003) 471–478; (b) V.R.K. Murthy, R. Raman, B. Vishwanathan, Proc. ICF-5 1 (1989) 447.
- [42] A.M. Sankpal, S.V. Kakatkar, N.D. Chaudhari, R.S. Patil, S.S. Suryavanshi, S.R. Sawant, J. Mater. Sci.-Mater. Electron. 9 (1998) 173.
- [43] S.S. Bellad, B.K. Chaugule, Mater. Res. Bull. 33 (1998) 1165.
- [44] K. Ohta, J. Phys. Soc. Jpn. 18 (1963) 685.
- [45] M. Drogenik, S. Besenicar, M. Lempel, Adv. Ceram. 16 (1985) 229.
- [46] M. Drogenik, Am. Ceram. Soc. Bull. 65 (1986) 656.
- [47] J. Loeac, J. Phys. D: Appl. Phys. 26 (1993) 963.
- [48] A. Globus, P. Duplex, Phys. Status Solidi 31 (1969) 765.
- [49] J. Smit, H.P.J. Wijn, in: L. Morton (Ed.), Ad. in Ele. and Ele. Phys., vol. VI, Academic Press, Inc. Publication, NY, 1954, p. 69.
- [50] G.P. Kramer, Y.I. Panova, Phys. Status Solidi A 77 (1983) 483.
- [51] J. Smit, Magnetic Properties of Materials, McGraw-Hill Co., NY, 1971.
- [52] V.K. Babar, J.S. Chandal, Bull. Mater. Sci. 18 (8) (1995) 997.